Supplementary Information

Table S1. Climate variables used to build demographic niche model for the focal song sparrow population. Abbreviations of the variable names and the range of values for each monthly climate variables as produced by ClimateNA for 2010-2018 are provided below.

Variable	Abbreviation	Min	Max
August Precipitation (mm)	Aug PPT	0	178.8
February Degree Days < 0°C	Feb DD < 0	0	94.8
December Degree Days < 0°C	Dec DD < 0	0	104.6
July Degree Days > 18 °C	Jul DD > 18	0	81
March Precipitation (mm)	Mar PPT	0	142.9
June Precipitation (mm)	Jun PPT	0	83
June Degree Days > 18 °C	Jun DD > 18	0	67.3

Table S2. Summary of climate variables used to model climate niche of song sparrows in the study area. Abbreviations of the variable names and the range of values for each variable during winter and breeding season as produced by ClimateNA for 2010-2018 are provided below.

		Resident		Migratory	
Variable	**Abbreviation**	**Min**	**Max**	**Min**	**Max**
Mean Temperature (°C)	Tave	-27.2	16.1	-18.1	32.8
Max. Temperature (°C)	Tmax	-22.9	23.8	-16.2	41.3
Min. Temperature (°C)	Tmin	-31.4	12.0	-20.5	24.4
Precipitation (mm)	PPT	0	1198.2	0	787.2
Degree Days < 0°C	DD < 0	0.8	803.3	0	383.2
Degree Days > 5°C	DD > 5	0	325.9	0	841.2
Degree Days > 18 °C	DD > 18	0	30.7	0	440.7
Number of Frost-Free Days	NFFD	0	29.5	0	30.5
Relative Humidity	RH	38.9	98.8	36.6	100.0
Precipitation as Snow (mm)	PAS	0	1178.9	0	601.3

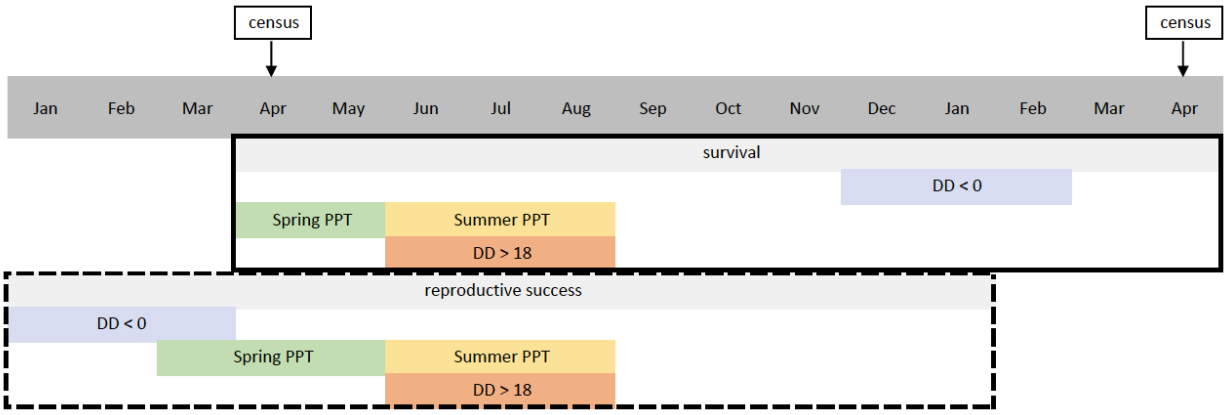

Figure S1. A timeline showing when variables used in the demographic models were measured. A census of the population took place every April in which all birds on the island were counted. Adult survival was measured between censuses and juvenile survival was measured between the time of fledging and the next census. Colored variables represent climate variables hypothesized to influence vital rates.

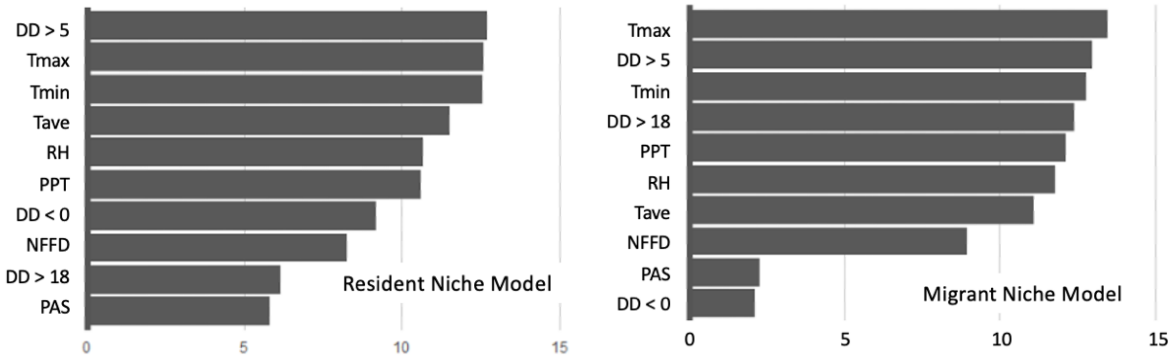

Fig S2. The variable importance of climate used in the climate niche models. Variables are ordered by ranked importance, as the mean decrease in model accuracy (DMA) in percent.

Table S3. Formulas and GLM model output for vital rate models used to calculate the demographic niche model.

Vital Rate	GLM Formula	Output	RMSE	Variable	Estimate	SE	Variable Importance
Adult Survival	Aug PPT + Feb DD < 0 + (Feb DD < 0)^2 + Dec DD < 0	F(4,41) =12.89, $p < 0.001$, $R^2 = 0.56$	0.359	Aug PPT	0.134	0.059	2.281
				Feb DD < 0	-0.065	0.086	2.201
				(Feb DD < 0)^2	-0.331	0.082	3.883
				Dec DD < 0	0.112	0.061	1.825
Juvenile Survival	Aug PPT + Feb DD < 0 + (Feb DD < 0)^2 + Dec DD < 0 + Jul DD > 18 + (Jul DD > 18)^2	F(6,39) =5.14, $p < 0.001$, $R^2 = 0.44$	0.598	Aug PPT	0.254	0.105	2.413
				Feb DD < 0	0.057	0.137	1.757
				(Feb DD < 0)^2	-0.457	0.106	2.568
				Dec DD < 0	0.190	0.109	1.735
				Jul DD > 18	-0.390	0.125	1.699
				(Jul DD > 18)^2	0.195	0.133	1.097
Reproductive Success	Mar PPT + Jun PPT + Jun DD >18	F(3,43) =8.49, $p < 0.001$, $R^2 = 0.47$	0.365	Mar PPT	0.151	0.055	2.749
				Jun PPT	0.175	0.059	2.929
				Jun DD > 18	0.207	0.059	3.498

Table S4. Predictive performance metrics used to compare the predictions to the actual observations from unseen data (out-of-bag samples): OOB error, sensitivity, specificity, AUC, and Kappa for the climatic niches of resident and migrant song sparrows.

Model	OOB error	Sensitivity	Specificity	AUC	Kappa
Resident niche model	0.155	0.811	0.784	0.886	0.591
Migrant niche model	0.139	0.830	0.803	0.896	0.626

Table S5. Climatic variables used to define climate space of the study area and loadings of each variable on the first two principal component axes that explained 78% of the variation (PC1: 56.2%; PC2: 21.8%). Monthly data from ClimateNA for the contemporary period (2010-2018) during the winter season (Jan – Feb) were aggregated into averages. See Fig. S3 for maps of the loading of PC1 and PC2.

Variable	Loadings	
	PC1	PC2
Tmax	0.407	0.049
Tmin	0.412	-0.054
Tave	0.412	-0.002
PPT	0.224	-0.486
DD_0	-0.389	0.11
DD5	0.293	0.399
DD18	0.193	0.33
NFFD	0.373	0.182
PAS	0.044	-0.519
RH	0.17	-0.419

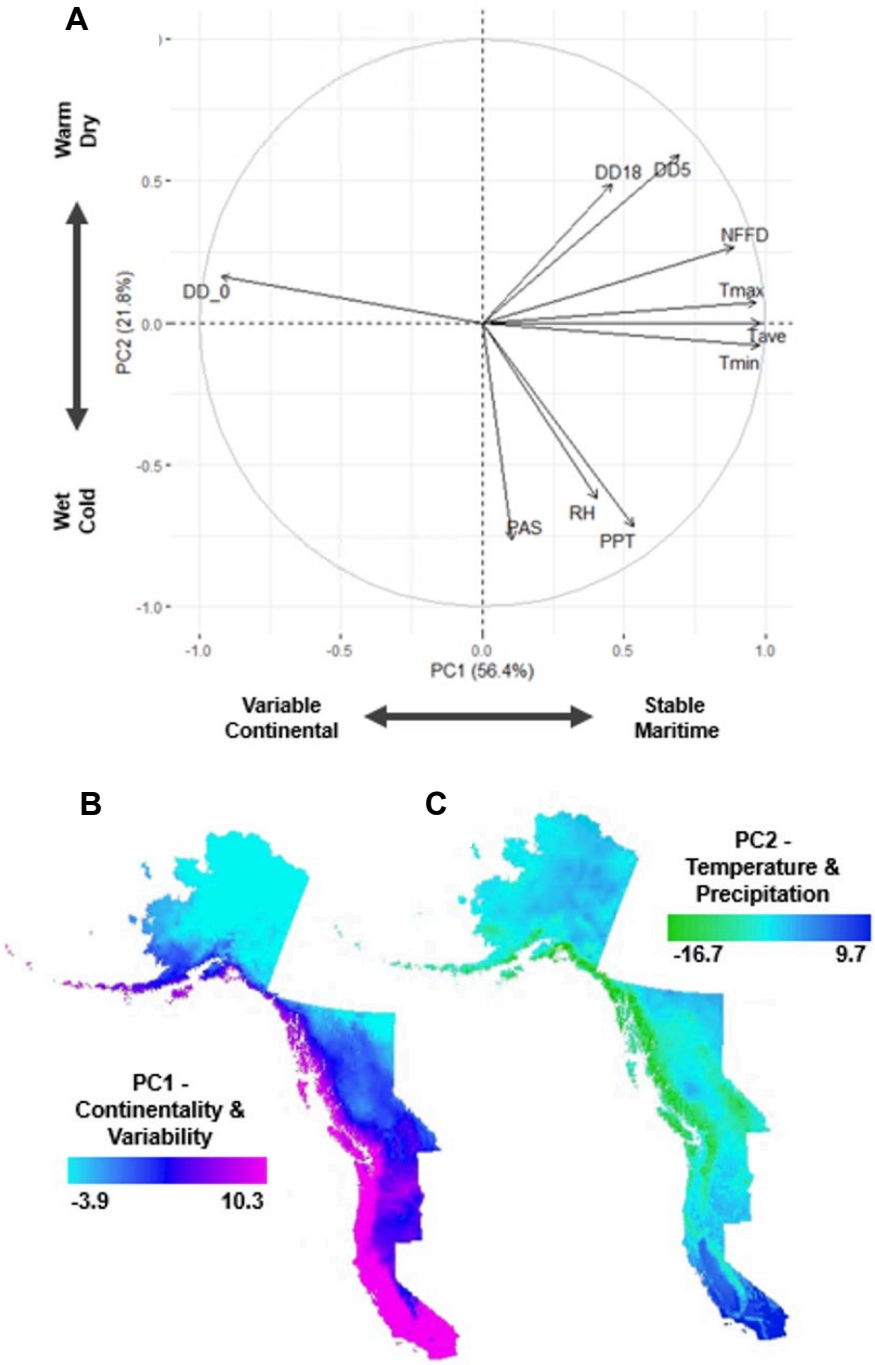

Figure S3. The primary climate gradients in the study area identified through a principal component analysis of the contemporary climate variables during winter. (A) Biplot of the climate gradients of variability and continentality, and temperature and precipitation, as represented by components (PC) 1 and 2. Spatial distribution of the variability and continentality gradient scores (B; PC1), and temperature and precipitation gradient scores (C; PC2). Coastal areas scored higher than their adjacent continental

space, suggesting that PC1 describes the continentality for an area. Variables were standardized prior to the PCA so that each one has mean zero and unit variance independent of its scale to ensures that all variables have the same weight in the analysis. Abbreviations of the climate variables shown in the biplot (A) are explained in Table S2.

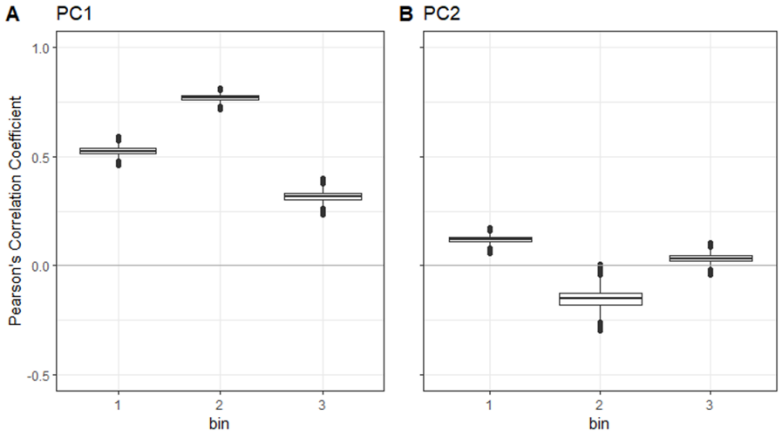

Figure S4. The estimated Pearson's correlation (*r*) of predictions from the contemporary resident climate niche model and demographic model of the study region grouped in bins where climate is considered similar. PC1 (A) and PC2 (B) represents variability and continentality gradient scores and temperature and precipitation gradient scores, respectively.

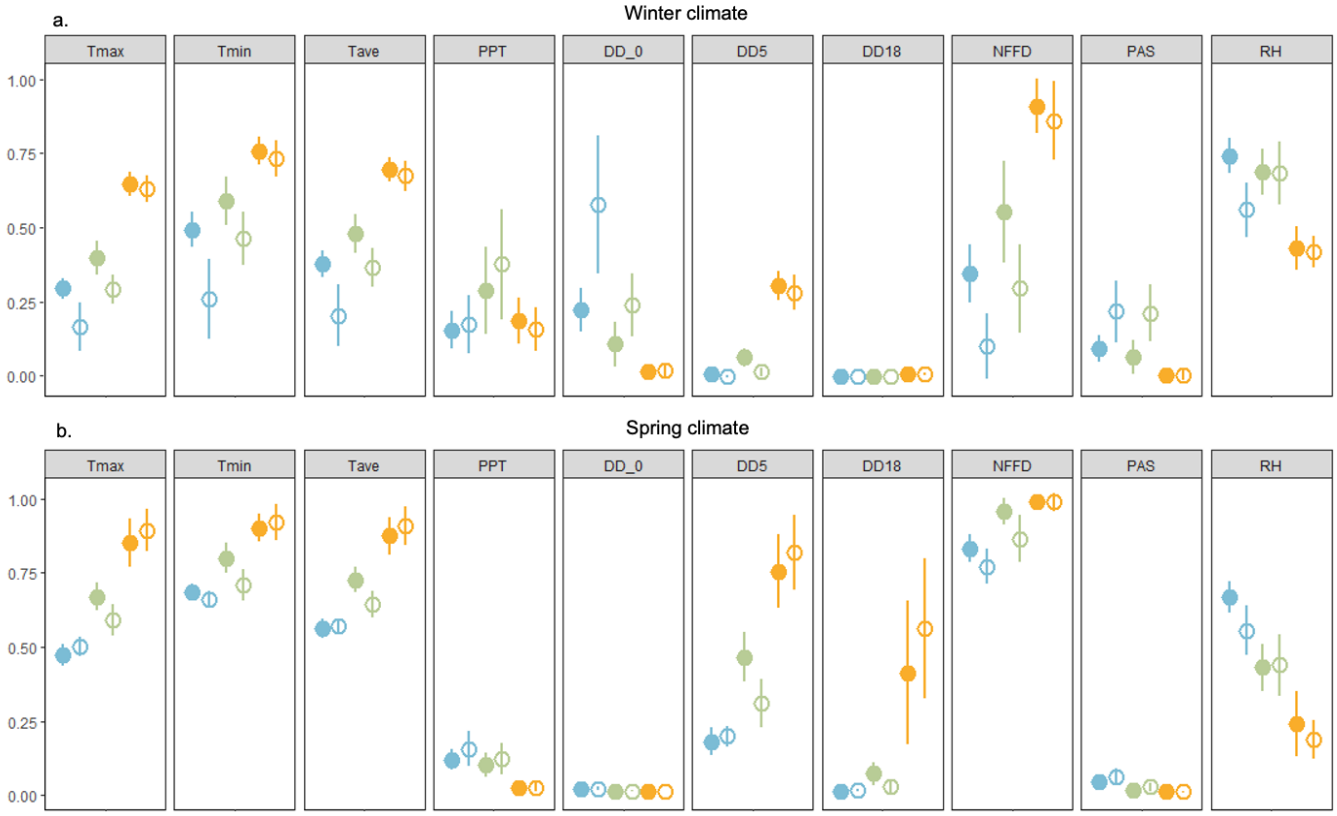

Figure S5. Variation (mean ± SD) in the variables used in the Climate Niche Model by inset locations shown in figure 1 in winter (a) and spring (b): Aleutian Islands, AK (blue), Georgia Basin, BC (green), and San Francisco Bay, CA (yellow). Filled and open circles represent the resident and migratory niches, respectively. To facilitate visual comparison variables were normalized to bring values to range from 0-1 by subtracting the minimum and dividing by the maximum and sampled randomly within each location and each niche (n = 5,000 per niche per location).

Table S6. F-statistics from the analysis of variance (ANOVA) used to describe the mean and range of variation in the contemporary migrant and resident niche climate variables. Raw climate variables used in the Climate Niche Model were randomly sampled by inset location shown in Figure 1 for each niche in winter and spring (n = 5,000 per niche per location). All values reported were significant at $p < 0.001$.

		Tmax	Tmin	Tave	PPT	DD < 0	DD > 5	DD > 18	NNFD	PAS	RH
winter	niche	17798.1	17377.3	18396.4	435.4	15747.7	4523.0	534.7	15236.1	15070.5	5175.2
	location	151961.0	48459.8	92755.8	6615.1	28785.7	210594.0	49615.7	70189.6	16228.0	32558.6
	niche:location	2956.4	3807.7	3450.5	671.9	6127.4	883.7	280.6	2106.6	3655.2	4153.2
spring	niche	6.7	3544.6	692.2	1889.1	1044.9	587.9	477.8	8089.6	3476.5	2870.7
	location	120860.0	69989.6	117301.1	22280.1	30045.1	115815.1	35998.3	35421.0	24387.3	55596.4
	niche:location	3546.6	3730.7	4171.3	532.9	271.3	4263.1	1291.9	2057.2	857.7	1340.2

Workflow & assumptions for demographic models

Our focal population is known to have high precision in estimates of survival, reproduction, and population growth due to high annual re-sighting probabilities (>99%; Wilson et al., 2007), enumeration of immigrants by color-banding (< 0.5 female/yr on average; Reid & Arcese 2020), and continuous monitoring of breeding activities. Thus, we calculate deterministic population growth rate as $\lambda = (Sj * RS) + Sa$, following Arcese & Marr (2006; see also Visty et al., 2018), assuming no further age structure or immigration. For simplicity, we only considered females when estimating demographic rates and population growth (Arcese et al., 1992; Arcese & Marr, 2006).

1. Response variables (S_a, S_j, RS) were mean-centered and natural-log transformed.
2. The full linear model included all variables in Table 1 (linear and second-order polynomial terms) with the transformed response variable from step 1.
3. We reduced the full model via supervised backward selection until only variables with $p < 0.1$ were remaining for our reduced models (Table S3). Model selection was also checked using corrected Akaike information criterion (AICc), which confirmed that in all cases our reduced models were one of the top two models selected.
4. Using *raster* package, we used our reduced models to predict these relationships across our study area. The resulting predictions were then back-transformed as follows:
   $e^{Sa - 0.6607}$
   $e^{Sj - 1.73617}$
   $e^{RS + 0.4596}$
5. Assuming that vital rates cannot exceed the mean ± 3 SE of our focal population on Mandarte, Island, we constrained the predicted values as follows:
   S_a: 0 – 0.99
   S_j: 0 – 0.69
   RS: 0 – 4.34
6. Reduced models from Table S3 were used to predict historical and future λ in relation to climate following the same protocol.
7. Assuming that long-term persistence at a site can only be achieved via seasonal migration, all spatial predications of λ were classified as supporting a 'resident' population if the predicted value of λ given local climate in each pixel was ≥ 1 (i.e., resident demographic niche), or a 'migrant' population if λ < 1 (i.e., migrant demographic niche).
8. For each demographic model (S_a, S_j, and RS), we also calculated prediction error in R using *se.fit = TRUE* as an argument to the raster::*predict()* function. We then calculated prediction uncertainty of λ following standard propagation of error formulas (Fig. S6; Taylor, 1997), and calculated 95% confidence limits on λ as *fit ± 1.96 * se.fit*.

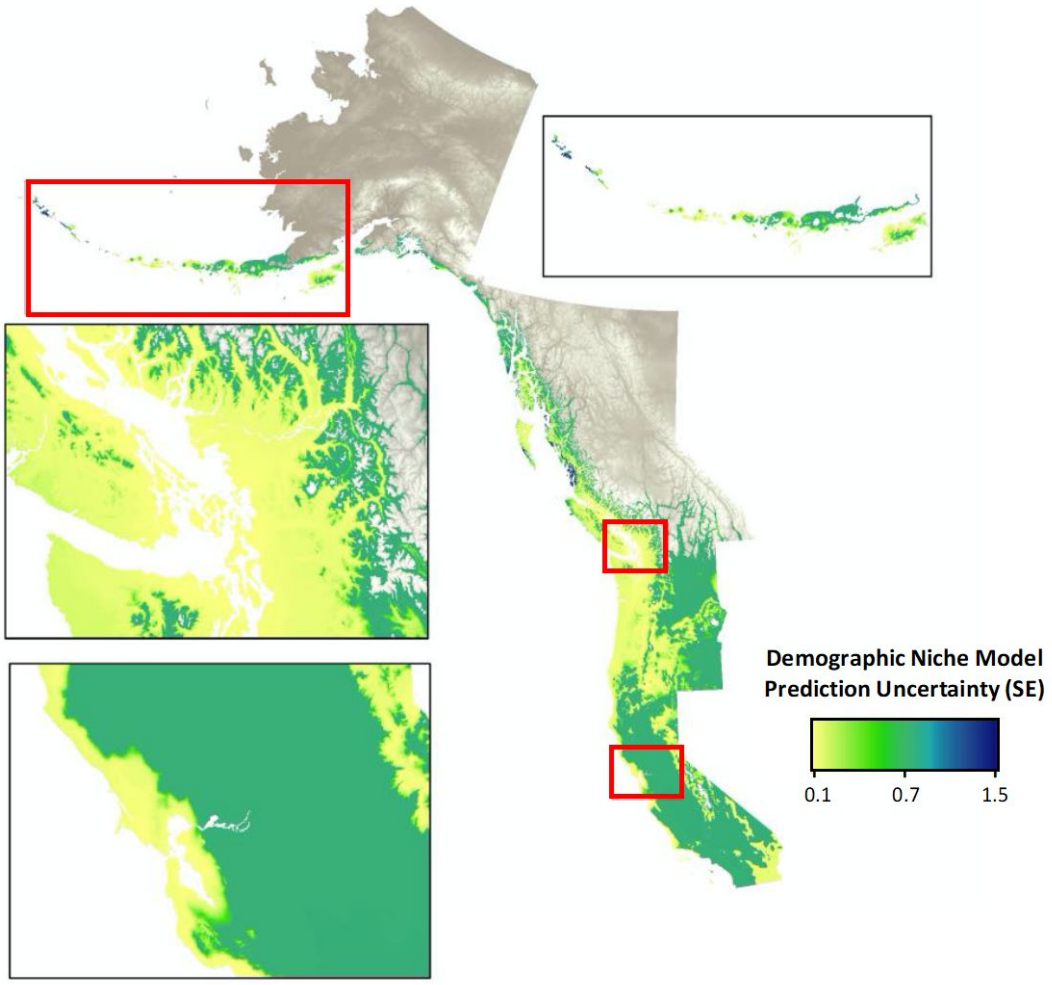

Figure S6. Demographic niche model prediction uncertainty (standard error; SE) across our study area. Insets indicate regions of interest: Aleutian Islands, AK, Georgia Basin, BC, and San Francisco Bay, CA.